Supplementary Material for

A novel PEC and ECL bifunctional aptasensor based on V_2CT_x MXene-derived MOF embedded with silver nanoparticles for selectively aptasensing miRNA-126

Yu Li[a], Shuai Zhang[b], Mengfei Wang[b], Chuanpan Guo[b], Zhihong Zhang[b*], Nan Zhou[a,*]

[a]Department of Orthopaedic Surgery, The First Affiliated Hospital of Zhengzhou University, Zhengzhou 450002, P. R. China

[b]College of Material and Chemical Engineering, Zhengzhou University of Light Industry, Zhengzhou 450001, P. R. China

* Corresponding authors

Email addresses: fcczhoun@zzu.edu.cn or 2006025@zzuli.edu.cn

Contents

S1. Experimental section

S1.1 Chemicals and reagents

Thioacetamide and *meso*-tetra(4-carboxyphenyl)porphine were purchased from Kaishu Chemical Technology Co., Ltd. (Shanghai, China). $InCl_3$ and $ZnCl_2$ were obtained from Shanghai Aladdin Biochemical Technology Co., Ltd (Shanghai, China). Ethanol and DMF were purchased from Luoyang Haohua Chemical Reagent Co., Ltd (Henan, China). All the chemicals are analytical reagent grade and used without further purification. Milli-Q water (18.2 Ω cm resistivity at 25 °C) was used throughout the experiments. The human breast cancer cell line (MCF-7) and mouse fibroblast cell line (L929) were obtained from the Cell Bank of the Chinese Academy of Sciences (Shanghai, China). All solutions were prepared with Milli-Q ultrapure water (≥18.2 MΩ·cm). cDNA, miRNA-126, miRNA-155, miRNA-122, miRNA-141, and miRNA-21, carcinoembryonic antigen (CEA), carbohydrate antigen 50 (CA50) were purchased from Qingke Biological Technology Co., Ltd. (Beijing, China). The base sequence of these DNA or RNA are listed as bellows

cDNA: 5'-CGC ATT ATT ACT CAC GGT ACG A-3'

miRNA-126: 5′-UCG UAC CGU GAG UAA UAA UGC G-3′

miRNA-155: 5′-UUA AUG CUA AUC GUG AUA GGG GUU-3′

miRNA-122: 5'-UGG AGU GUG ACA AUG GUG UUU G-3'

miRNA-141: 5′- UAA CAC UGU CUG GUA AAG AUG G -3′

miRNA-21: 5′- UAG CUU AUC AGA CUG AUG UUG A -3′

S1.2 Preparation of all solutions

In this work, phosphate buffer solution (PBS, 0.01 M, pH = 7.4) was used as the biological buffer, which was prepared by mixing 0.242 g KH_2PO_4, 1.445 g $Na_2HPO_4 \cdot 12H_2O$, 0.2 g KCl, and 8.003 g NaCl in Milli-Q water. The solution was then adjusted to pH 7.4 by adding 0.1 M HCl solution. The electrolyte solution was prepared immediately before use by dissolving 1.65 g $K_3Fe(CN)_6$, 2.11 g $K_4Fe(CN)_6 \cdot 3H_2O$ and 7.5 g KCl in PBS (1.0 L).

The stock solution of CDNA (100 nM), and miRNA solutions of different concentrations (10, 100, 1000, 10^4, 10^5, 10^6, and 10^7 fM) and other solution were prepared using 0.01 M PBS (pH 7.4) and stored at 4 °C.

S1.3. Basic characterizations

Power X-ray diffraction spectrometer (PXRD, Bruker D8 Advance, German) was used to characterize the crystal structure of photocatalyst. The microstructure and morphology of photocatalyst was analyzed by field emission scanning electron microscope (FE-SEM, regulus8100 Hitachi, Japan) and transmission electron microscope (TEM, JOEL2100f, JOEL Ltd, Japan). X-ray photoelectron spectroscopy (XPS, Thermo Fisher Scientific K-Alpha, USA) was used to analyze the surface chemical state of photocatalyst and the existing forms of elements. The FT-IR spectra were recorded by the Nicolet 6700 FT-IR spectrometer, and the scanning range is 4000–500 cm^{-1}. Raman spectra of the prepared catalysts were obtained on a Renishaw inVia Raman spectrometer with a solid-state laser (excitation at 532 nm) at room temperature in the range of 50−4000 cm^{-1}. UV photoelectron spectroscopy (UPS, VG Scienta R4000, British) is used to study work function. The adsorption-desorption isotherm of

nitrogen was measured by Autosorb-iQ instrument and analyzed by Bruner-Emmett-Taylor equation. The aperture was analyzed by Barrett-Joyner-Halenda (BJH). Ultraviolet-visible diffuse reflectance spectrum was measured by ultraviolet-visible spectrophotometer (UV-vis DRS, Solid Spec 3700, Japan), with Ba_2SO_4 as reference. The electron paramagnetic resonance (EPR) spectra were collected using a Bruker EMX EMXplus-6/1 spectrometer in the X-band frequency (≈9.826 GHz) with a field modulation frequency of 100 kHz. Optoelectronic properties of samples were measured on an electrochemical analyzer (CHI 660E, China) with a standard three-electrode system. The Ag/AgCl is used as reference electrode, the counter electrode is Pt plate, and the working electrode is FTO coated with photocatalyst. Transient photocurrent response and electrochemical impedance were measured using 0.5 M Na_2SO_4 as electrolyte solution.

S2. Basic characterizations of V-PMOF

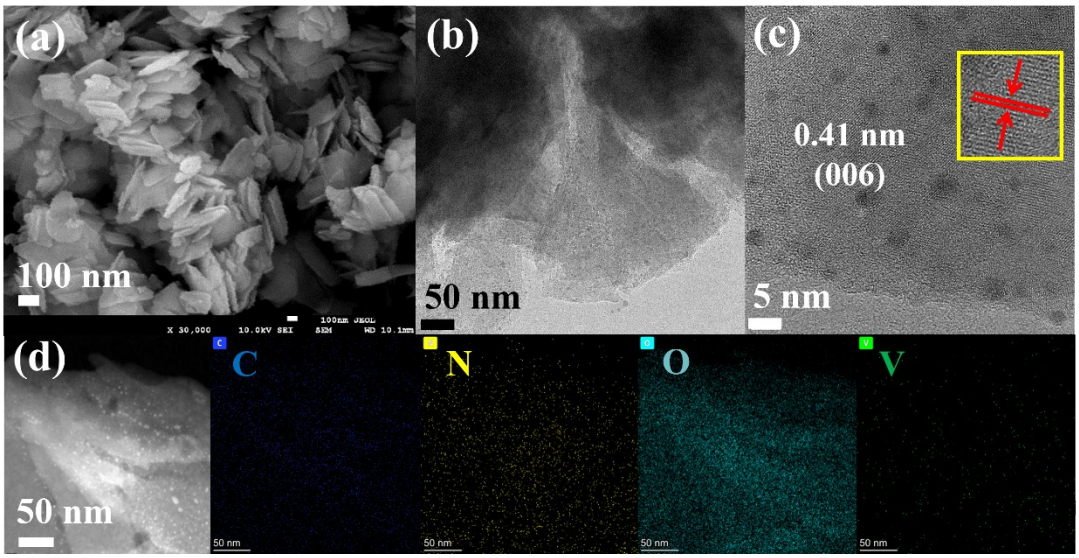

Fig. S1 (a) SEM, (b, c) low- and high-magnification TEM images, (d) HAAD-STEM image and corresponding EDS element mapping images of V-PMOF: C (blue), N (yellow), O (cyan) and V (red).

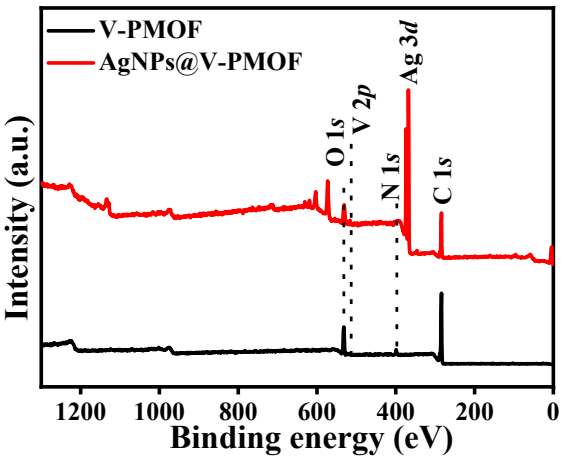

Fig. S2 XPS survey spectra of V-PMOF and AgNPs@V-PMOF.

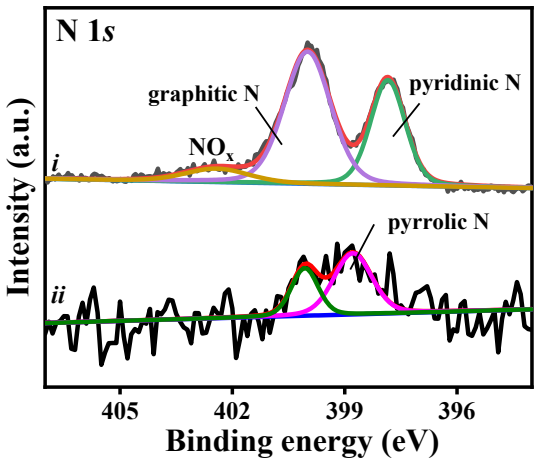

Fig. S3 High-resolution N 1*s* XPS spectra of (*i*) V-PMOF and (*ii*) AgNPs@V-PMOF.

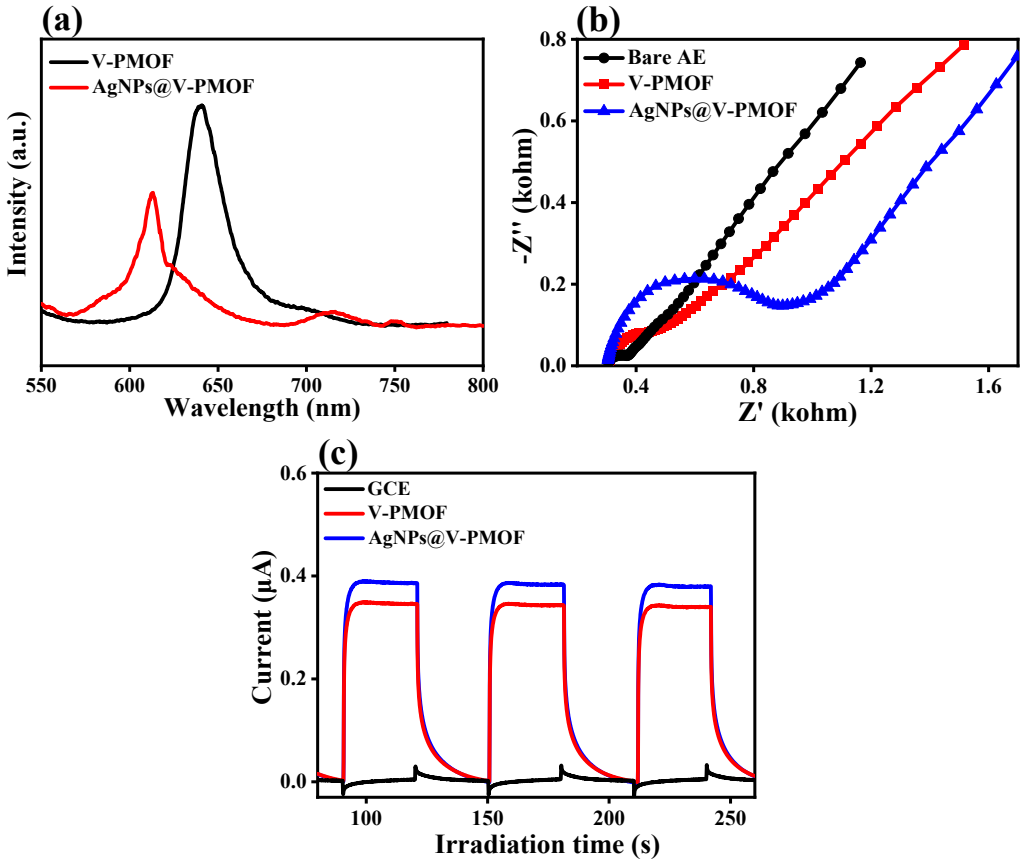

Fig. S4 (a) PL spectra, (b) EIS Nyquist plots, and (c) photocurrent responses of V-PMOF and AgNPs@V-PMOF.

S3. Detection of miRNA-21 using the AgNCs@V-PMOF-based biosensor

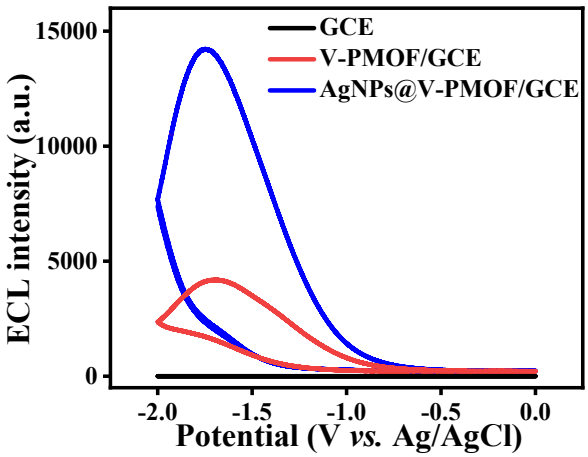

Fig. S5 (a) ECL-potential profiles of bare GCE, V-PMOF/GCE, and AgNCs@V-PMOF/GCE in a 5 mM $S_2O_8^{2-}$ (scan range of –2.0 to 0 V, *vs.* Ag/AgCl).

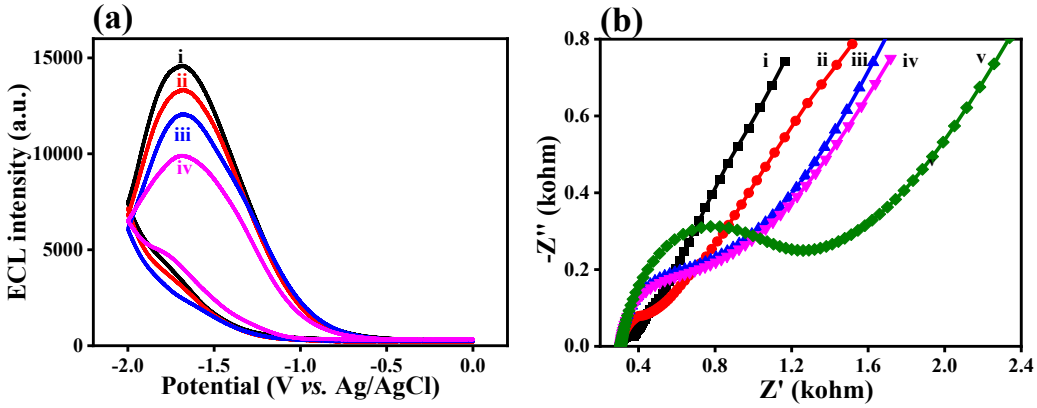

Fig. S6 (a) ECL-potential profiles of (i) AgNCs@V-PMOF/GCE, (ii) cDNA/AgNCs@V-PMOF/GCE, (iii) BSA/cDNA/AgNCs@V-PMOF/GCE, and (iv) miRNA-126/BSA/cDNA/AgNCs@V-PMOF/GCE in 5 mM $S_2O_8^{2-}$ solution (scan range of –2.0 to 0 V, *vs.* Ag/AgCl). (b) EIS Nyquist plots of (i) bare GCE, (ii) AgNCs@V-PMOF/GCE, (iii) cDNA/AgNCs@V-PMOF/GCE, (iv) BSA/cDNA/AgNCs@V-PMOF/GCE, and (v) miRNA-126/BSA/cDNA/AgNCs@V-PMOF/GCE in 0.01 M PBS containing 5 M $[Fe(CN)_6]^{3-/4-}$ redox.

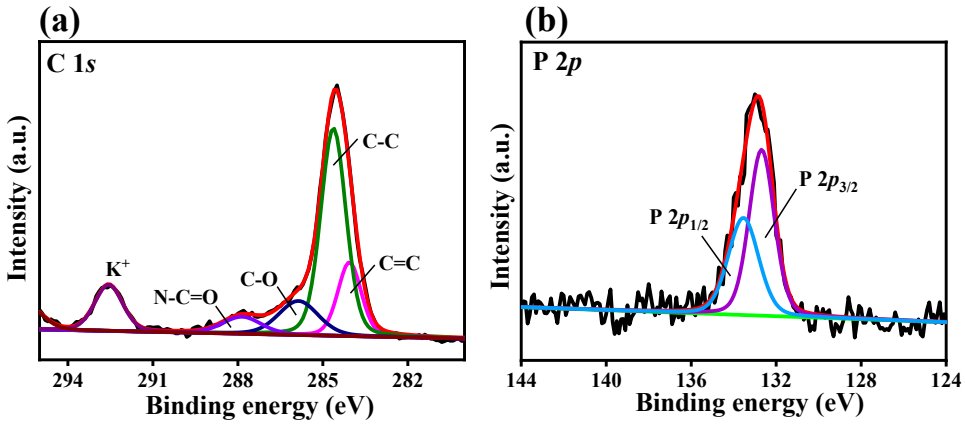

Fig. S7 High-resolution XPS spectra of (a) C 1*s* and (b) P 2*p* of cDNA/AgNPs@V-PMOF.

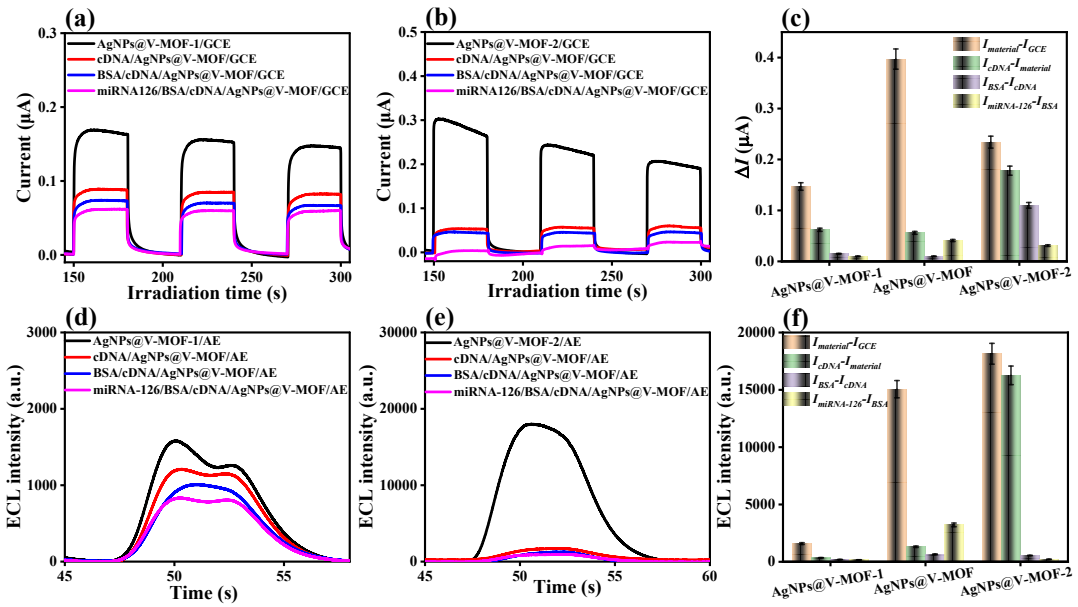

Fig. S8 Photocurrent responses of the (a) AgNPs@V-PMOF-1 and (b) AgNPs@V-PMOF-2-based aptasensor for the detection of miRNA-126. (c) The Δ*I* values for each stage of miRNA-126 detection with PEC aptasensors based on AgNPs@V-PMOF-1, AgNPs@V-PMOF and AgNPs@V-PMOF-2. ECL intensities of the (d) AgNPs@V-PMOF-1 and (e) AgNPs@V-PMOF-2-based aptasensor for the detection of miRNA-126. (f) The Δ*I* values for each stage of miRNA-126 detection with ECL aptasensors based on AgNPs@V-PMOF-1, AgNPs@V-PMOF and AgNPs@V-PMOF-2.

The detection of miRNA-126 was then performed by the PEC and ECL aptasensor constructed using these two hybrids as the electrode materials (**Figs. S8**). **Fig. S8c** illustrated that the used AgNPs@V-PMOF had the highest PEC response among the three samples. This result reveal that the maximum photocurrent was achieved when the addition of $AgNO_3$ was 5 mg, which is enough to improve the performance of PEC. In addition, the presence of excess Ag NPs would prevent the efficient absorbance of light. As shown in **Fig. S8f**, the ECL response of the hybrid increased with increasing the dosage of Ag NPs in the AgNPs@V-PMOF hybrid. It can be contributed to the

surface Plasmon resonance effect of Ag NPs, accelerated electron transfer and promoted the photocarrier density. Notably, the AgNPs@V-PMOF-based apatsensor demonstrated the largest ΔI obtained from the detection of miRNA-126, indicating its best sensing performance. Therefore, the AgNPs@V-PMOF was selected as the sensing material for the construction of the PEC and ECL aptasensor to detect miRNA-126.

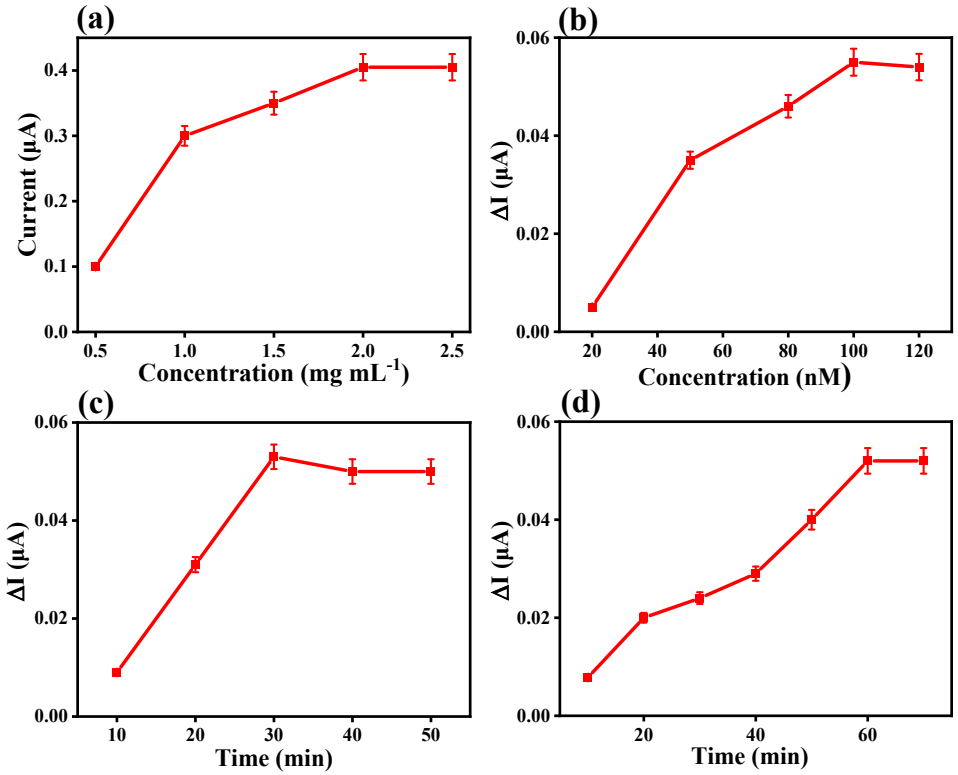

Fig. S9 (a) Influence of AgNCs@V-PMOF dosage (0.5, 1, 1.5, 2 and 2.5 mg mL^{-1}) on the current values of the modified electrodes. (b) Influence of aptamer strands concentration (20, 50, 80, 100, and 120 nM), (c) the incubation time of aptamer, and (d) the binding time of miRNA-126 on the current values of the AgNCs@V-PMOF-based PEC biosensors.

Fig. S9a depicted that the obtained PEC responses obtained by the detection of miRNA-126 (10 fM) separately using the series of biosensors constructed with different AgNPs@V-PMOF dosages. The gained PEC signal toward miRNA-126 increased with increasing the AgNPs@V-PMOF usage from 0.1 to 2 mg mL^{-1}. When the dosage of AgNPs@V-PMOF was larger than that of 2 mg mL^{-1}, the gained PEC response approached to platform. The optimal dosage of the sensitive layer was set as 2 mg mL^{-1}. **Fig. S9b** displayed the level of miRNA-126 detected using the PEC biosensors

constructed by anchoring diverse concentrations of cDNA strands. Distinctly, the obtained response was up to a platform for the detection of miRNA-126 when the anchored cDNA concentration over the modified electrode was higher than 100 nM. Thereby, the optimal cDNA concentration was set as 100 nM for further constructing the used biosensors. Moreover, the influence of the adsorption time of cDNA over the AgNPs@V-PMOF/GCE on the detection of miRNA-126 was illustrated in **Fig. S9c**. The result revealed an equilibrium was achieved when the incubation time was up to 0.5 h. **Fig. S9d** indicated the hybridization time of miRNA-126 and cDNA immobilized over the developed biosensor showed that the obtained PEC responses reached an equilibrium at 1 h.

Table S1 Comparison of the AgNCs@V-PMOF-based biosensor for the detection of miRNA-126 with other reported sensors

Materials	Detection method	Detection range	LOD	Refs.
Fe_3O_4@SiO_2@AuNPs	ECL	5 fM – 5000 fM	2 fM	[1]
PDA-PBA NPs@MoS_2 nanosheet	ECL	1 aM–1 nM	0.56 aM	[2]
PycDs@MSX	ECL	100 aM–100 pM	13.0 aM	[3]
Microchip electrophoresis	Microchip electrophoresis	0.025 nM–20 nM	15 pM	[4]
Microfluidic system	Field-effect transistor (FET) detection system	1 fM–1000 fM	23.82 fM	[5]
PAMAM-Au-Ag nanocomposite	Electrochemical analysis	1.0 fM–10 nM	0.79 fM	[6]
AgNPs@V-PMOF	**PEC**	**1 fM – 1 nM**	**0.78 fM**	**This work**
	ECL	**0.1 fM - 1 nM**	**0.05 fM**	

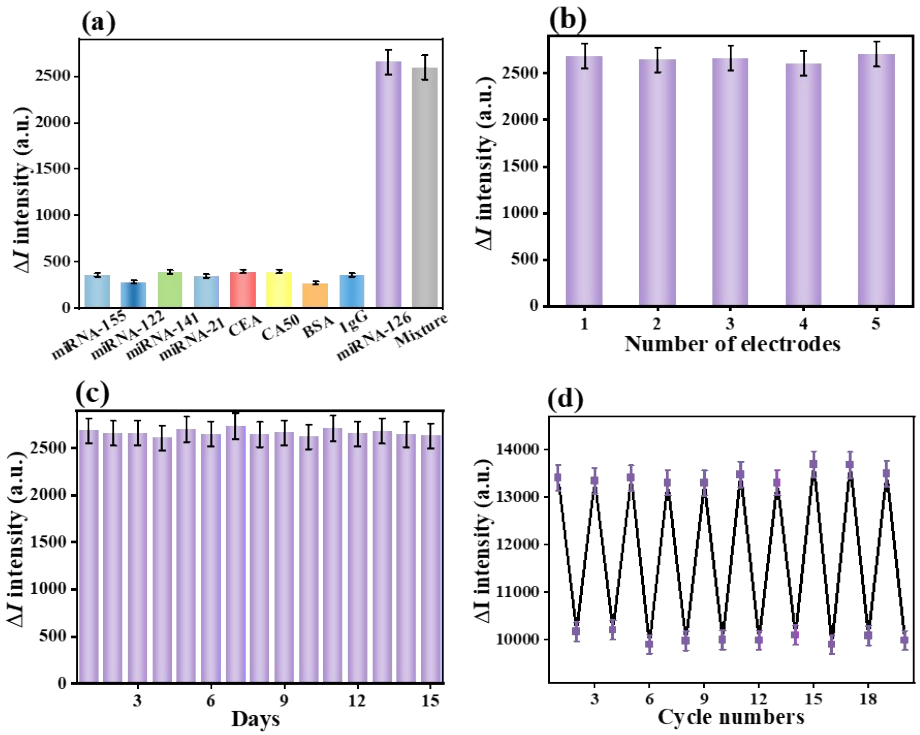

Fig. S10 (a) Selectivity of the constructed AgNPs@V-PMOF-based ECL biosensor for the detection of miRNA-126 (10 fM) in the presence of miRNA-155, miRNA-122, miRNA-141, miRNA-21, CEA, CA50 (1 pM), and their mixture with miRNA-126. (b) Reproducibility, (c) storage stability, and (d) regenerability of the developed AgNPs@V-PMOF-based ECL biosensor for the analysis of miRNA-126 (100 fM). The error bars represented average standard errors for three measurements (n = 3).

Table S2 Determination of miRNA-126 in human serum by the proposed ECL biosensor (n = 3).

Added amounts (fM)	**Found amounts (fM)**	**Recovery (%)**	**RSD (%)**
1	1.05	105.1	2.51
10	11.15	111.5	1.52
10^2	94.66	94.66	3.41
10^3	1111.58	111.58	3.58
10^4	9466.52	94.66	1.52
10^5	98322.15	98.32	2.41
10^6	1111588.41	111.58	1.48

Table S3 Determination of miRNA-126 in human serum by the proposed PEC biosensor (n = 3).

Added amounts (fM)	Found amounts (fM)	Recovery (%)	RSD (%)
1	1.09	109.4	1.87
10	9.83	98.3	2.58
10^2	105.96	105.96	1.34
10^3	1137.51	113.75	2.89
10^4	10937.87	109.38	1.56
10^5	95391.34	95.39	3.41
10^6	1153576.38	115.36	2.95

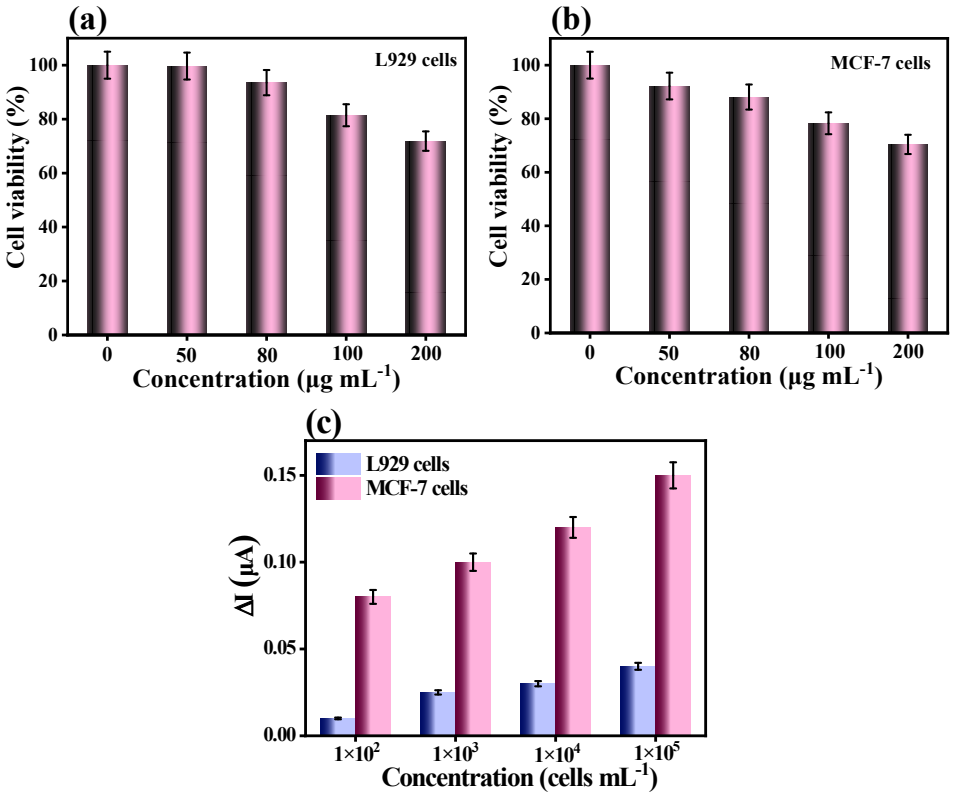

Fig. S11 Cell viability of the AgNPs@V-PMOF Schottky junction against (a) normal L929 cells and (b) cancer MCF-7 cells. (c) The variations in the current values for the detection of miRNA-126 containing in the normal L929 cells and living MCF-7 cells.

References

1 Y. Zheng, Y. Xu, L. Chen, X. Yin, F. Lin, S. Weng, X. Lin, *J. Electrochem. Soc.,* 2020, **167**, 167502.

2 X. Zhang, Y. Nie, Q. Zhang, Z. Liang, P. Wang, Q. Ma, *Chem. Eng. J.,* 2021, **411**, 128428.

3 T.-T. Tu, Y.-M. Lei, Y.-Q. Chai, Y. Zhuo, R. Yuan, *ACS Appl. Mater. Inter.,* 2020, **12**, 3945-3952.

4 K. Wei, J. Zhao, Y. Qin, S. Li, Y. Huang, S. Zhao, *Talanta,* 2018, **189**, 437-441.

5 H.-L. Cheng, C.-Y. Fu, W.-C. Kuo, Y.-W. Chen, Y.-S. Chen, Y.-M. Lee, K.-H. Li, C. Chen, H.-P. Ma, P.-C. Huang, Y.-L. Wang, G.-B. Lee, *Lab on a Chip,* 2018, **18**, 2917-2925.

6 L. Liu, S. Jiang, L. Wang, Z. Zhang, G. Xie, *Microchim. Acta,* 2015, **182**, 77-84.